

Inverse-photoemission spectroscopy of GaSe and InSe

R. Sporcken,* R. Hafsi, F. Coletti, and J. M. Debever

Groupe de Physique des Etats Condensés, Université Aix-Marseille II, Case 901, F-13288 Marseille Cedex 9, France

P. A. Thiry

Laboratoire Interdisciplinaire de Spectroscopie Electronique, Facultés Universitaires Notre Dame de la Paix, Rue de Bruxelles 61, B-5000 Namur, Belgium

A. Chevy

Physique des Milieux Condensés, Université Pierre et Marie Curie, 75252 Paris Cedex 05, France

(Received 6 August 1993)

The lamellar semiconductors GaSe and InSe have been studied with k -resolved inverse-photoemission spectroscopy along two major symmetry directions ($\bar{\Gamma}\bar{K}$ and $\bar{\Gamma}\bar{M}$) of the surface Brillouin zone. Three bands with well-resolved features are observed from which the dispersion of the conduction bands can be determined with good precision. The minimum of the conduction band is found at \bar{M} in GaSe and at $\bar{\Gamma}$ in InSe. These results are compared with theoretical studies using pseudopotential and tight-binding calculations.

I. INTRODUCTION

The electronic properties of the semiconductor compounds GaSe and InSe have received considerable attention during the last two decades because of their quasi-two-dimensional character. The layered structure of these compounds is due to the strong covalent intralayer bonds as opposed to the very weak Van der Waals-type interlayer bonds. As a result, the electronic band structure of the valence and conduction bands is expected to show only little dispersion versus k_{\perp} , where k_{\perp} is the electron wave-vector component perpendicular to the surface. This fact was used by Smith and Traum¹ to demonstrate the possibility of mapping the valence-band structure of solid materials from angle-resolved-photoemission experiments. Recent experiments² on the epitaxial growth of layers of C_{60} on layered compounds have stimulated renewed interest in this class of materials. Indeed it appears that the weak Van der Waals interlayer bonding plays an important role in achieving long-range order in these layers of C_{60} .

Although the optical properties and the valence-band structure of GaSe have been studied in much detail, little has been published about its conduction-band structure. In one experimental study of the conduction-band structure of GaSe,³ the experiment's geometry restricted the available information to the $\bar{\Gamma}\bar{M}$ direction, whereas a more recent work was plagued by sample charging.⁴ On the other hand, theoretical calculations of the conduction-band structure relevant to our work are the tight-binding results by Doni *et al.*⁵ and Robertson,⁶ and the pseudopotential calculations by Schlüter and co-workers^{7,8} and Depeursinge.⁹ Because direct measurements of the conduction-band dispersion were not available when these calculations were made, they had to be tested against indirect results from experiments such as optical-absorption spectroscopy or photoluminescence spectroscopy.¹⁰ In this work we present a direct mea-

surement by inverse-photoemission spectroscopy of the conduction-band structure of GaSe and InSe in two directions of high symmetry. The results will be compared with theoretical calculations, and the respective merits and weaknesses of the tight-binding and pseudopotential methods will be addressed.

Even less is known about the conduction-band structure of InSe. A study of the valence-band structure by Larsen, Chiang, and Smith¹¹ is worthwhile mentioning here, especially since they pointed out an asymmetry of the peak intensities in the valence-band spectra with respect to the sign of k_{\parallel} along $\bar{\Gamma}\bar{M}$. A similar behavior will be described for the conduction bands of GaSe and InSe in the present paper. To the best of our knowledge, no inverse-photoemission data have been published for InSe. Information about the electronic band structure of this material is available from photoconductivity,¹² Bremsstrahlung-isochromat spectroscopy,¹³ and electron-energy-loss spectroscopy.¹⁴ These latter experiments produced very similar spectra for InSe and GaSe, suggesting that the electronic structure of these compounds is very similar as well.

The present paper is organized as follows. First we describe the experimental setup used for the measurement of inverse-photoemission spectra, as well as the sample preparation. We then turn to a discussion of the experimental results, starting with a qualitative description of the inverse-photoemission spectra of GaSe and InSe. Particular care was taken in the determination of accurate transition energies in the spectra in order to obtain reliable conduction-band dispersion curves. This procedure will be described. We then discuss the energy dispersion of the conduction-band states along $\bar{\Gamma}\bar{M}$ and $\bar{\Gamma}\bar{K}$ and compare our experimental results to theoretical calculations. An interesting result is the asymmetry of the experimental energy dispersion along two opposite azimuths $\bar{\Gamma}\bar{M}$ and $\bar{\Gamma}\bar{M}'$ [i.e., $E(k_{\parallel}) \neq E(-k_{\parallel})$ for some states and some values of k_{\parallel} along $\bar{\Gamma}\bar{M}$]. This effect is

similar to a recent observation for Si(111),¹⁵ though much weaker, and has important practical implications on the determination of the nature and magnitude of the optical gap in these compounds.

II. EXPERIMENT

The k -resolved inverse-photoelectron spectroscopy (KRIPES) experiments are performed in an ultrahigh vacuum chamber pumped by an ion getter pump and a liquid-nitrogen-cooled Ti-sublimation pump. Low-energy electron-diffraction (LEED) and Auger-electron spectroscopy facilities are available in the same chamber. The collimated beam of low-kinetic-energy electrons (7–17 eV, angular divergence $\leq 3^\circ$) for KRIPES is produced by an electron gun with a BaO cathode. In order to check for sample charging, the target current was varied from 0.5 to 5 μA . Only those samples for which the KRIPES spectra were insensitive to the target current were used for this study. Typical target currents for a complete series of spectra were between 1 and 2 μA at 17-eV kinetic energy.

KRIPES spectra are measured at an isochromat energy of 9.5 eV using a Geiger-Müller type detector. Ultraviolet photons emitted by the radiative decay of “free” electron states into lower conduction-band states are focused by elliptic mirrors ($f=1$) onto a SrF₂ window. The overall energy resolution of the spectrometer is 0.35 eV. The position of the Fermi level is measured from the cutoff of the emission from a clean tantalum foil, which can be readily exchanged with the sample.

For a given sample orientation, the conduction-band dispersion with k_{\parallel} is investigated by rotating the electron gun, on either side of the sample normal, in a vertical plane perpendicular to the sample (i.e., by scanning the polar angle θ). The sample can also be rotated about a vertical axis, making it possible to probe two orthogonal directions during the same experiment (fixed sample, rotating electron gun, and vice versa). The configuration with the sample kept in place and the electron gun rotating is normally preferred because it has less effect on the focusing of the mirror. In order to check that the spectra are free from drift, about 5–10 normal-incidence spectra are recorded over the course of the measurement of a series of KRIPES spectra for one azimuth.

The GaSe (InSe) samples are mounted with conductive silver paint on metallic sample holders. Since the materials studied here are layered compounds, they are easily cleaved *in situ*. For this purpose, an adhesive tape is attached to the sample surface. The sample is then loaded into the vacuum system and the tape pulled off carefully, taking with it a thin sheet of GaSe (InSe). In this process, care must be taken to make sure that the sheet which is left exposed after cleaving is still in electrical contact with the silver paint and thus with the sample holder, in order to avoid electrostatic charging of the sample when it is irradiated by the electron beam. Indeed we observed that because of the weakness of the Van der Waals interlayer bonds, the cleaving procedure sometimes leaves a sheet on the sample which is only loosely attached to the sample in some points. Such samples tend to charge dur-

ing the measurements, making it impossible to obtain reliable energy positions for the conduction bands. These difficulties with the cleaving could be related to the presence of impurities between some layers in the samples. The samples for this experiment were screened before they were introduced into the spectrometer, and only those samples producing good cleaved surfaces were used. As a result, the spectra presented here were not affected by electrostatic charging.

Prior to the measurements, the azimuthal orientation of the sample is established with the help of LEED. The sample normal is then determined by measuring the target current: an extremum occurs in the target current when the incident electron beam is exactly normal to the sample. This technique gives a precision of $\pm 0.5^\circ$. The electron gun is rotated with the same precision.

III. DATA ANALYSIS

The IPE data are stored as a set of spectra, one for each angle of incidence of the electrons; each spectrum represents the photon count rate versus final-state energy E_f with respect to the Fermi level E_F . In order to determine reliable conduction-band dispersion curves from such a collection of spectra, we must locate all the features in the spectra to the highest possible accuracy. For this purpose, the spectra are first normalized with respect to the incident electron-beam current. They are then fitted to the sum of N Gaussians, added to an empirical background. The parameters for the Gaussians (height, width, position) are adjusted with an optimization procedure based on the simplex algorithm. The background is due to photons from radiative transitions by electrons which have already lost some energy in inelastic collisions. This is the pendant to the secondary electron background in ultraviolet photoemission spectroscopy. It is approximated here by a sequence of typically three or four linear segments determined manually. The position of the Gaussians is almost independent of the shape of the background (less than ± 100 -meV variation), whereas the intensities are of course affected significantly, especially on the high-energy side of the spectrum. Since our interest is in peak positions, this approximation for the background is sufficient. It should also be pointed out that the sharpness of the features in the conduction-band spectra makes it easy to use such a procedure.

In addition to the normal verification of convergence and consistency of the solution, other safeguards are used to make sure a meaningful fit is obtained. Gaussians are included in the fit only if they can be related to a visible feature in the spectrum, such as a peak, shoulder or asymmetry. A fit is rejected if it yields a Gaussian with a width smaller than the resolution or with a negative height. Finally, the number of Gaussians should be independent of the angle of incidence of the electrons, at least over a limited range. After the positions of the Gaussians have been determined for all the spectra, the electron wave-vector component parallel to the surface is computed using the relation

$$k_{\parallel} \sim (E_{\text{kin}})^{1/2} \sin \theta, \quad (1)$$

where E_{kin} is the kinetic energy of the incoming electron giving rise to a transition in the spectra, and θ is the corresponding angle of incidence of the electrons with respect to the surface normal.

IV. RESULTS

A. GaSe

For a description of the crystal structure of GaSe and of the corresponding Brillouin zone and its points of high symmetry, we refer the reader to the existing literature.¹⁶ KRIPES spectra for GaSe were recorded for various directions of the incident electron beam in the $\Gamma ML A$ and $\Gamma KH A$ planes of the Brillouin zone, referred to as the $\Gamma \bar{M}$ and $\Gamma \bar{K}$ directions, respectively. Figure 1 shows such a set of spectra, plotted as normalized photon intensity versus final-state electron energy relative to the Fermi level. Discrete symbols are raw data normalized with respect to the incident-beam current, whereas the solid lines represent the fit according to the procedure described in Sec. III. Small vertical ticks indicate the position of the Gaussians used for the fits. For the spectra at -50° , the decomposition into individual Gaussians is shown.

Three groups of peaks are present in each set of spectra, located around 2–3, 4–6, and 6–9 eV, respectively.

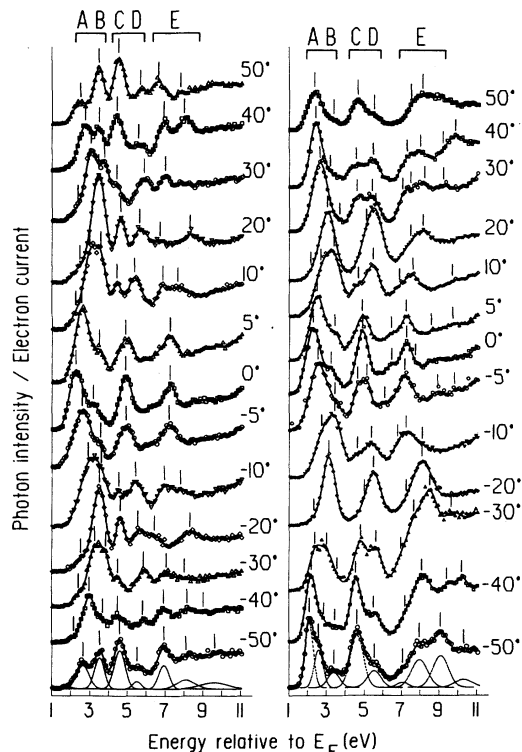


FIG. 1. k -resolved inverse photoemission spectra of GaSe recorded at $h\nu=9.5$ eV as a function of polar angle along the $\Gamma \bar{M}$ (left panel) and $\Gamma \bar{K}$ (right panel) directions. The vertical bars indicate the position of the main peaks determined by the curve-fitting procedure described in the text. For the spectra at -50° , the decomposition into individual peaks is shown.

Remarkably sharp features are observed and the signal is almost zero between the bands. This reflects the localized character of the density of states due to the weak interaction between layers. These compounds can thus be viewed as a system intermediate between isolated molecules and a three-dimensional solid.

For both sets of spectra, the energy dispersion of these features is rather symmetrical with respect to the spectrum for normal incidence. This is also true for the relative intensities of the peaks in the spectra for the $\Gamma \bar{K}$ direction, whereas for the $\Gamma \bar{M}$ direction there are significant differences between the relative peak heights for positive and negative values of θ . This asymmetry shall be addressed below when we discuss the conduction-band dispersion curves.

The agreement between fit and data is remarkably good. Particular care was taken to keep the fitting procedure as operator-independent as possible, which gives strong confidence in the resulting dispersion curves. In core-level photoelectron spectroscopy, it is common practice to use curve fitting to obtain precise values for the binding energies, but we are not aware of any similar reports for the localization of features in the valence-band photoelectron spectra or in inverse-photoelectron spectra from conduction bands. The result in Fig. 1 shows that, at least in some cases, curve fitting is very useful for the analysis of KRIPES data.

Strictly speaking, the use of a Gaussian line shape for the fits is an approximation. It is clear that lifetime broadening should add a Lorentzian contribution, and the instrumental broadening is not exactly Gaussian either. However, with an instrumental resolution of 0.35 eV, a detailed analysis of the line shape does not seem realistic, especially for the lowest conduction bands for which the measured width is only slightly larger than the instrumental resolution. In order to keep the number of fitting parameters reasonably low, and since we are extracting only peak positions, we use the approximation of a Gaussian line shape. We note, however, that the width of the features in the spectra increases with increasing energy, probably because of the shorter lifetime of the states at higher energy, due to the larger number of possible deexcitation channels.

In Fig. 2, the energies $E(k_{\parallel})$ of the features in Fig. 1 are shown as a function of $|k_{\parallel}|$. Circles correspond to spectra for negative values of θ , while triangles correspond to positive values of θ . The solid lines are results from theoretical calculations in the literature and will be discussed below. $\bar{K}\bar{M}$ is the extension of $\Gamma \bar{K}$ into the second Brillouin zone. The good match at $\bar{\Gamma}$ and—to the extent where data are available—at \bar{M} for both directions $\Gamma \bar{M}$ and $\Gamma \bar{K}\bar{M}$ gives an idea about the experimental accuracy in this work. As already mentioned in earlier parts of this paper, the data are nearly perfectly symmetrical with respect to $k_{\parallel}=0$ in the $\Gamma \bar{K}$ direction, whereas some differences between the dispersion curves for $k_{\parallel}<0$ and $k_{\parallel}>0$ are seen along $\Gamma \bar{M}$, particularly for the lowest conduction bands. This asymmetry along $\Gamma \bar{M}$ cannot be explained by invoking a systematic error in the measurement of the polar angle θ . Indeed, a simple shift of the origin $k_{\parallel}=0$ does not make the dispersion curves symme-

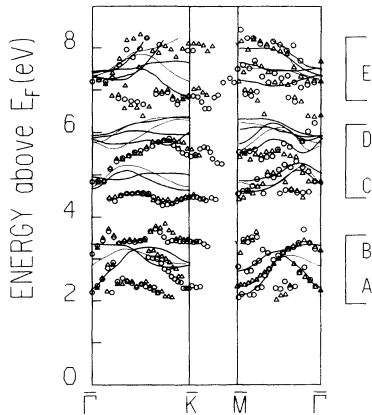


FIG. 2. Comparison between the measured band structure of GaSe, determined from the spectra of Fig. 1, and a theoretical band structure from the pseudopotential calculations by Schlüter (Refs. 7 and 8). For details on how the theoretical band structure is extracted from both Refs. 7 and 8, see text. Circles correspond to experimental data for negative values of θ , while triangles correspond to positive values of θ . Bold solid lines are theoretical results for the ΓM and ΓK directions, thin lines are for AH and AL .

trical. In fact, not only the shape but also the number of observed bands is unequal on either side of $\bar{\Gamma}$: in the lower set of conduction bands, three branches are seen between \bar{M} and $\bar{\Sigma}$ for negative values of θ , while only two branches are found for positive values of θ . A similar effect has already been reported earlier for inverse-photoemission spectroscopy on H-Si(111) (1×1).¹⁵ As already stated by those authors, the asymmetry is not due to the conduction-band structure itself, but to the way it is probed by KRIPES. The results of Fig. 2 are directly related to the projection of the bulk conduction-band structure onto the surface. Obviously, such a projected band structure does not depend on the sign of k_{\parallel} , but the matrix elements which determine the strength of the transitions between empty states can depend on the sign of k_{\parallel} , because of the symmetry of the crystal structure of GaSe. As a result, some states may not be probed with equal weight along k_{\parallel} and $-k_{\parallel}$; some states may even be visible along k_{\parallel} and invisible along $-k_{\parallel}$, and vice versa. For GaSe, KRIPES spectra depend on the sign of k_{\parallel} along $\bar{\Gamma M}$ and not along $\bar{\Gamma K}$. This can be understood because only $\bar{\Gamma K}$ is perpendicular to a mirror plane for the crystal structure of GaSe, not $\bar{\Gamma M}$. Obviously, this explanation supposes that the conduction bands show some dispersion with k_{\perp} . Incidentally, this gives an indication of the order of magnitude of the dispersion with k_{\perp} which must be comparable to the asymmetry of the energy dispersion along $\bar{\Gamma M}$ (a few hundred meV).

Experimentally, we observe a small energy difference between the lowest conduction bands at $\bar{\Gamma}$, \bar{K} , and \bar{M} . Relative to $\bar{\Gamma}$, the lowest conduction band lies 80 ± 50 meV higher at \bar{K} , and 130 ± 50 meV lower at \bar{M} . Between $\bar{\Gamma}$ and \bar{K} , there is also a band at about 130 meV below the minimum at $\bar{\Gamma}$, but this band is not seen close to \bar{K} . It is important to note that the minimum of the lowest con-

duction band at \bar{M} is found for negative values of θ , whereas this band is found slightly above its position at $\bar{\Gamma}$ for positive values of θ . This is due to the asymmetry discussed above. It is therefore important to explore both sides of the surface Brillouin zone in order to locate the minimum of the conduction band. At any rate, we deduce that GaSe is a semiconductor with an indirect gap corresponding to a transition between the top of the valence band at $\bar{\Gamma}$ and the conduction band at \bar{M} or at a point near \bar{K} . The direct transition at $\bar{\Gamma}$ is about 130 meV larger. This is in good agreement with previous KRIPES results⁴ as well as with the conclusion from photoluminescence studies,¹⁷ although this latter work yielded a smaller difference (25 meV) between the absolute minimum of the conduction band at \bar{M} and the relative minimum at $\bar{\Gamma}$.

For a comparison with our experimental data, we have chosen three different theoretical works which agree at least partially with the experiment. These calculations use either a pseudopotential method⁷⁻⁹ or a semiempirical tight-binding scheme.^{5,6} In a first version of Schlüter's pseudopotential study,⁷ the band structure of GaSe was obtained up to 6 eV above the bottom of the conduction band. Later, he modified⁸ the theoretical band structure essentially by increasing the Ga-Ga spacing from the experimental value of 2.39 Å to twice the covalent radius of Ga (2.52 Å) in order to account for new experimental data from ultraviolet-photoemission, X-ray-photoemission, and reflectivity measurements. However, results of this latter calculation were cut off at 4 eV above the bottom of the conduction band. Therefore, we combine the lower bands (up to 3 eV above the bottom of the conduction band) from the more recent and supposedly improved calculation with the upper bands from the earlier pseudopotential calculation. A comparison with the experiment is shown in Fig. 2. Circles and triangles are KRIPES data for opposite signs of k_{\parallel} respectively, bold solid lines are theoretical results for the ΓM and ΓK directions, and thin lines are for AH and AL .

For the lowest group of conduction bands, the agreement is excellent between $\bar{\Gamma}$ and $\bar{\Gamma M}$, although some experimentally observed features are not predicted by theory. One additional state (A in Fig. 2) near the bottom of the conduction band is seen around $\bar{\Sigma}$, while another is found close to \bar{M} at about 3.3 eV. Between $\bar{\Gamma}$ and \bar{K} , the differences are somewhat more pronounced for the same group of bands, but the overall agreement is still very good. Again, an unpredicted state is seen near the bottom of the conduction band. Moreover, the pair of states which is predicted to be degenerate at \bar{K} , is split into two bands (B in Fig. 2) in the experiment, and the largest separation occurs at \bar{K} .

Band C is still in reasonable agreement, although it is found about 0.5 eV below the theoretical curve along $\bar{\Gamma K}$. The shape of band D also agrees reasonably well with the experiment, except near $\bar{\Gamma}$ where it does not rise fast enough. Moreover, the splitting between the two branches of band D seems too large compared to the experiment. Considering the larger experimental uncertainties at higher energies due to lower signal-to-noise ratio, and given the fact that, according to the author of the

calculations,⁷ the upper conduction bands should only be considered approximate, it is almost surprising that there are no major discrepancies for band *E* along $\bar{\Gamma}\bar{M}$. Along $\bar{\Gamma}\bar{K}$, bands *D* are too high compared to the experiment, and the lowest band of group *E* is too high around $\bar{\Gamma}$.

Without performing more theoretical calculations, it is difficult to explain the differences between theory and experiment. We can, however, give some suggestions for the modifications which might lead to an improved agreement, and hence to a better understanding of the conduction-band structure of GaSe. First, we point out that the calculations are performed for β -GaSe, while the samples are probably $\epsilon+\gamma$ polytypes. Furthermore, the experiment probes the projection of the bulk conduction-band structure onto the surface, while the calculations yield the bulk band structure along selected lines of high symmetry. Fortunately for this study, the interaction between layers in the lamellar material GaSe is weak. Therefore, we expect to see errors due to these effects of a few 100 meV at most, which, however, is insufficient to explain some of the discrepancies.

Starting with direction $\bar{\Gamma}\bar{M}$, we observe band *A* up to 700 meV away from the nearest calculated band, depending on k_{\parallel} . This is somewhat large compared to the expected magnitude of the aforementioned effects, raising the question of whether or not this state is truly a bulk state of GaSe. However, as we will see, tight-binding calculations indeed predict a rather flat state at this energy, ruling in favor of a true GaSe state. Also, the lowest calculated state of group *B* is rather sensitive to changes in the parameters for the pseudopotential calculations. This can be seen by comparing both versions of Schlüter's calculations. We thus suggest that band *A* is part of the GaSe band structure, and is simply not well accounted for by the existing pseudopotential calculations.

It is not too difficult to suggest a correction for the large theoretical splitting between the two branches of band *D*. This splitting is related to the strength of the interaction between adjacent layers in GaSe. According to Schlüter, this interaction is overestimated in the calculated band structures. A repulsive term should therefore be included in the interlayer potential; this might then bring the splitting in line with the experiment. Along $\bar{\Gamma}\bar{K}$, theory and experiment are more difficult to reconcile. A first step might be to increase the number of plane waves in the calculations. This is expected to decrease the gaps between groups of bands and thus to lower bands *C* and *D*, bringing them closer to the experimental bands.

Figure 3 shows a comparison of our experimental data with a pseudopotential calculation by Depeursinge.⁹ The calculated curves were shifted arbitrarily along the vertical axis in order to obtain the best "overall agreement" between experiment and theory. Incidentally, this places the Fermi level slightly above the top of the valence band, as expected for this type of sample.

The main difference between theory and experiment here is that some of the calculated bands disperse more strongly than in the experiment. For example, the large splitting in the calculated bands *C* between $\bar{\Gamma}$ and \bar{K} is not seen in the experiment. However, contrary to Schlüter's calculations, these bands are now predicted to

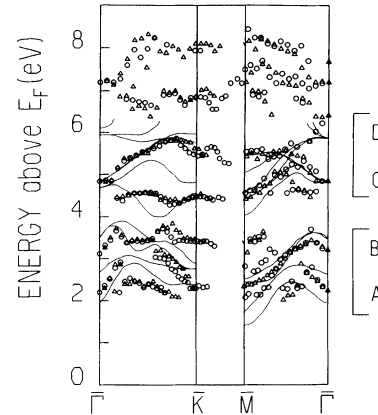


FIG. 3. Comparison between the measured band structure of GaSe, determined from the spectra of Fig. 1, and a theoretical band structure from the pseudopotential calculations by Depeursinge (Ref. 9). Circles correspond to experimental data for negative values of θ , while triangles correspond to positive values of θ . The theoretical results for the *AH* and *AL* directions are shown together with the results for the $\bar{\Gamma}\bar{M}$ and $\bar{\Gamma}\bar{K}$ directions.

be degenerate at $\bar{\Gamma}$, in agreement with the experiment. Furthermore, band *A* is now predicted by the theory, confirming our suggestion that the weak feature near the conduction-band minimum in the spectra of Fig. 1 is really due to a state in the conduction-band structure of GaSe. However, the experiment suggests that the dispersion of this state might be overestimated in the calculation.

Regarding the nature of the gap in GaSe, this calculation predicts the minimum of the conduction band at \bar{M} , but the difference with the relative minimum at $\bar{\Gamma}$ is much larger than the experimental value.

We now turn to a brief comparison between our KRIPES data and the semiempirical tight-binding calculations by Doni *et al.*⁵ Figure 4 shows the experimental data together with the calculated conduction-band dispersion curves in a presentation similar to that of Figs. 2 and 3. Obviously, the overall agreement is not very good. This can easily be understood because tight-binding calculations are known to give an insufficient description of conduction bands. However, it is particularly interesting to note that the relatively flat state (*A*) near the bottom of the conduction band is predicted by those calculations, although it was missing in the pseudopotential calculation by Schlüter. The strongly dispersing state *B* is missing in these tight-binding calculations. It has been shown¹³ that such a state can be obtained by including atomic excited Se 5s orbitals in the tight-binding scheme. Regarding the bands above 4 eV, it is possible to imagine relatively simple though major distortions which would match them reasonably well to the experiment. Specifically, reducing the dispersion of the upper bands along $\bar{\Gamma}\bar{M}$ by raising them about 0.5–1 eV near $\bar{\Gamma}$ would improve the agreement in this direction. We conclude that, although tight-binding calculations do not reproduce the shape of the conduction bands of GaSe, they can help to explain some of their qualitative

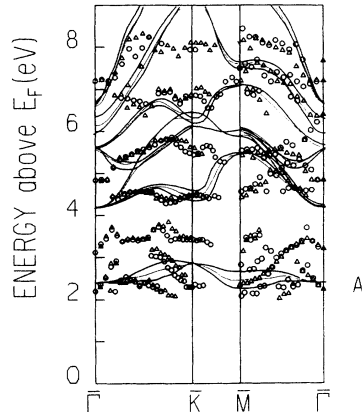


FIG. 4. Comparison between the measured band structure of GaSe, determined from the spectra of Fig. 1, and a theoretical band structure from tight-binding calculations by Doni *et al.* (Ref. 5). Circles correspond to experimental data for negative values of θ , while triangles correspond to positive values of θ . Bold solid lines are theoretical results for the ΓM and ΓK directions, thin lines are for AH and AL .

features such as the nature, number, and sequence of bands or their approximate energies.

B. InSe

For the discussion of the experimental KRIPES results on InSe, we start again with a series of KRIPES spectra for various directions of the incident electron beam in the $\Gamma ML A$ and $\Gamma KH A$ planes of the Brillouin zone, referred to as the ΓM and ΓK directions, respectively (Fig. 5). As for GaSe, the spectra for the ΓK direction are remarkably symmetrical with respect to $k_{\parallel}=0$, while there are some differences between spectra for $k_{\parallel}<0$ and $k_{\parallel}>0$ along ΓM . This asymmetry is strongest for the lowest conduction bands. It is particularly evident on the spectra for $\theta=\pm 15^{\circ}$ and $\pm 20^{\circ}$. Once again, we propose that this symmetry is due to the dependence of the matrix elements for transitions between states in the conduction band on the sign of k_{\parallel} .

The energy of the features in the spectra of Fig. 5 is determined by the fitting procedure described in an earlier part of this paper. The result is shown in Fig. 6 as a plot of $E(k_{\parallel})$ versus $|k_{\parallel}|$. Circles correspond to spectra for negative values of θ , while triangles correspond to positive values of θ . The solid lines are results from the pseudopotential calculation by Depeursinge.⁹ The calculated bands have been shifted along the energy axes in order to reach good agreement with the lowest measured conduction bands. All the observed bands are predicted by the calculation, and the overall agreement is remarkably good. Only the highest bands are found to be significantly higher than in the calculation, but the theory is not expected to produce accurate results for states so far above the conduction-band minimum, and the experiment is limited by low signal-to-noise ratio in this area.

For the lowest conduction bands, the agreement is excellent, except near \bar{K} where the calculated bands are all located at about 2 eV while the experiment shows three

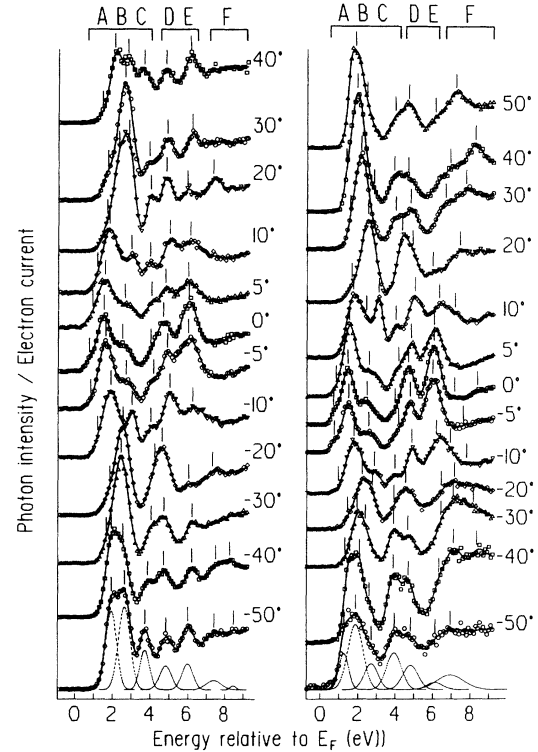


FIG. 5. k -resolved inverse photoemission spectra of InSe recorded at $h\nu=9.5$ eV as a function of polar angle along the ΓM (left panel) and ΓK (right panel) directions. The vertical bars indicate the position of the main peaks determined by the curve-fitting procedure described in the text. For the spectra at -50° , the decomposition into individual peaks is shown.

clearly distinct bands at about 1.5, 2, and 2.7 eV. This could be due in part to some dispersion with k_{\perp} , although the amount of this dispersion is expected to be somewhat smaller. Both the experiment and theory predict InSe to be a semiconductor with a direct band gap. Although the

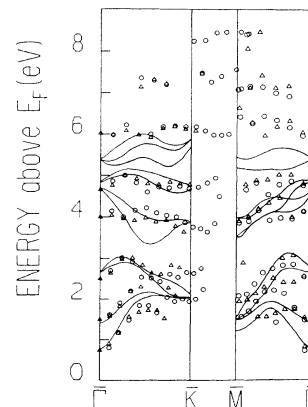


FIG. 6. Comparison between the measured band structure of InSe, determined from the spectra of Fig. 5, and a theoretical band structure from the pseudopotential calculations by Depeursinge (Ref. 9). Circles correspond to experimental data for negative values of θ , while triangles correspond to positive values of θ . The theoretical results are obtained for the ΓM and ΓK directions, as well as for AH and AL .

electronic band structure of InSe is qualitatively similar to the one of GaSe in most respects, this is a main difference since we have shown that GaSe has an indirect band gap, even though for GaSe the separation is small between the lowest conduction bands at Γ , M and K . Combining our measured conduction bands with the valence band structure measured by Larsen, Chiang, and Smith,¹¹ we find a separation of 3 eV between the highest valence band and the lowest conduction band at K , compared to 3.6 eV between the highest valence band and the second conduction band at K . This information might help to reassign some transitions in the optical absorption or reflectivity spectra on InSe.

V. CONCLUSIONS

We have measured k -resolved inverse-photoemission spectra of GaSe and InSe along two major symmetry directions ($\bar{\Gamma}\bar{K}$ and $\bar{\Gamma}\bar{M}$). Three bands with sharp features are observed around 2–3, 4–6, and 6–9 eV for GaSe, and around 1–3, 4–5, and 6–8 eV for InSe. Curve fitting was used to locate the transitions in the spectra, and the projected conduction-band structure was determined. The data are nearly perfectly symmetrical with respect to $k_{\parallel}=0$ in the $\bar{\Gamma}\bar{K}$ direction, whereas some differences between the dispersion curves for $k_{\parallel}<0$ and $k_{\parallel}>0$ are seen along $\bar{\Gamma}\bar{M}$, particularly for the lowest conduction bands. We attribute this asymmetry to the dependence of the matrix elements for transitions between states in the conduction band on the sign of k_{\parallel} . This effect is thus related to the symmetry of the GaSe and InSe crystals, and to the three-dimensional character of their band structure. The magnitude of the asymmetry was used to estimate the dispersion of the conduction bands with k_{\perp} .

We find that the conduction-band structures of GaSe and InSe are very similar. The main difference between the two compounds is that InSe is a semiconductor with a direct band gap, while GaSe has an indirect band gap corresponding to a transition between the top of the valence band at Γ and the conduction band at M or at a point near K . The direct transition at Γ is about 130 meV larger. The minimum of the lowest conduction band at \bar{M} is found for negative values of θ , whereas this band is found slightly above its position at $\bar{\Gamma}$ for positive values of θ . This means that for GaSe, it is important to measure KRIPES spectra for both positive and negative polar angles in order to determine the nature of the band gap.

The measured conduction-band structures were compared with theoretical band structures from tight-binding and pseudopotential calculations for GaSe, and with results from pseudopotential calculations for InSe. Tight-binding calculations can only explain some of the qualitative features of the band structure, whereas we find very good agreement between the experimental band structure and pseudopotential calculations. KRIPES probes transitions between excited states of negatively charged atoms in a solid. Since the agreement with the pseudopotential calculations (corresponding to neutral atoms) is good, we conclude that the effect of the additional negative charge on the shape and the relative position of the bands is small in this particular case.

ACKNOWLEDGMENTS

R.S. acknowledges financial support from the Belgian National Fund for Scientific Research. We would like to thank Professor J. P. Vigneron for helpful discussion. "Groupe de Physique des Etats Condensés" is URA 783 of CNRS.

*Permanent address: Facultés Universitaires Notre Dame de la Paix, Laboratoire Interdisciplinaire de Spectroscopie Electronique, Rue de Bruxelles 61, B-5000 Namur, Belgium.

¹N. V. Smith and M. M. Traum, Phys. Rev. B **11**, 2087 (1975).

²G. Gensterblum, L. M. Yu, J. J. Pireaux, P. A. Thiry, R. Caudano, J. M. Themlin, S. Bouzidi, F. Coletti, and J. M. Debever, Appl. Phys. A **56**, 175 (1993).

³J. M. Nicholls and J. M. Debever, Surf. Sci. **189**, 919 (1987).

⁴F. Coletti, R. Hafsi, and J. M. Debever, J. Lumin. **48-49**, 645 (1991).

⁵E. Doni, R. Girlanda, V. Grasso, A. Balzarotti, and M. Piacentini, Nuovo Cimento **51B**, 154 (1979).

⁶J. Robertson, J. Phys. C **12**, 4777 (1979).

⁷M. Schlüter, Nuovo Cimento **13B**, 313 (1973).

⁸M. Schlüter, J. Camassel, S. Kohn, J. P. Voitchovsky, Y. R. Shen, and M. L. Cohen, Phys. Rev. B **13**, 3534 (1976).

⁹Y. Depeursing, Nuovo Cimento **64B**, 1111 (1981).

¹⁰E. Mooser and M. Schlüter, Nuovo Cimento B **18**, 164 (1973).

¹¹P. K. Larsen, S. Chiang, and N. V. Smith, Phys. Rev. B **15**, 3200 (1977).

¹²O. Z. Alekperov, M. O. Godjaev, M. Z. Zarbaliev, and R. A. Suleimanov, Solid State Commun. **77**, 65 (1991).

¹³B. Smandek, Y. Gao, T. J. Wagner, J. H. Weaver, F. Lévy, and G. Margaritondo, Phys. Rev. B **37**, 4196 (1988).

¹⁴H. Araki, S. Nishikawa, T. Tanbo, and C. Tatsuyama, Phys. Rev. B **33**, 8164 (1986).

¹⁵S. Bouzidi, F. Coletti, J. M. Debever, P. A. Thiry, P. Dumas, and Y. J. Chabal, Phys. Rev. B **45**, 3 (1992).

¹⁶E. Doni and R. Girlanda in *Electronic Structure and Electronic Transitions in Layered Materials*, edited by V. Grasso (Reidel, Dordrecht, 1986), pp. 1–171.